Full-Duplex Coherent Analogue mm-wave RoF Transmission with Simplified RRH and Photonic Down-Conversion of Uplink

Bernhard Schrenk[(1)], Aina Val Marti[(1)], Thomas Zemen[(1)], and Fotini Karinou[(2)]

[(1)]AIT Austrian Institute of Technology, 1210 Vienna, Austria. Author e-mail: bernhard.schrenk@ait.ac.at
[(2)] Microsoft Research Ltd., Cambridge CB1 2FB, United Kingdom.

Abstract: We demonstrate full-duplex analogue transmission of mm-wave radio at 29.3/34.3GHz using an EML to simultaneously perform coherent downlink detection and uplink transmission at the RRH. We further introduce photonic down-conversion of the uplink to simplify its frequency translation while eliminating *dispersion-induced fading over 15km reach.*

Introduction

Beyond-5G radio networks seek for elevated carrier frequencies to boost the wireless capacity while enabling new deployment scenarios such as mm-wave backhauls in fiber-scarce plants or heterogeneous radio networks augmented by small cells performing beam-centric communication to realize a high-rate data shower [1]. Towards this direction, the simplification of the remote radio head (RRH) as the distributed field element of radio access networks calls for analogue radio-over-fiber (RoF) techniques [2]. Earlier works have proposed photonic up-conversion techniques to several RF bands [3-10], remote modulation schemes [11] or coherent transceiver elements based on electro-absorption modulated lasers (EML), which up to now has only been proven to support full-duplex radio transmission in the sub-6GHz band, yet over a single wavelength [12] and even a single RF carrier frequency [13].

In this work, we advance coherent analogue RoF transmission with a full-duplex EML transceiver as simplified optical RRH interface to the mm-wave band and prove, for the first time, that the same methodology enables optical frequency translation at the central office (CO), thus reducing its complexity by omitting RF down-conversion and making the analogue RoF transmission robust to dispersion-induced fading. We prove these points through full-duplex radio transmission at 34.3/29.3 GHz over an optical budget of 18.7 dB and a 15 km reach.

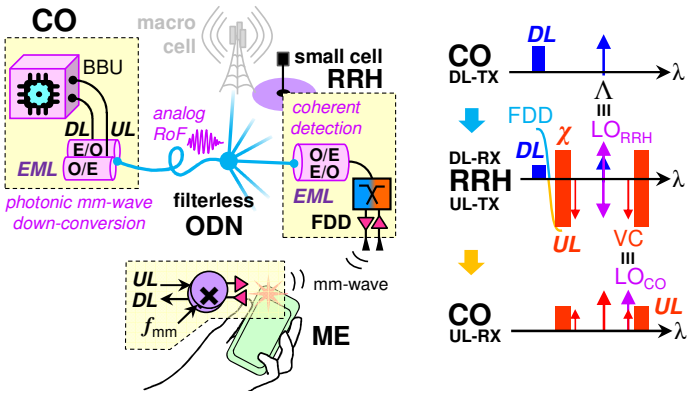

Fig. 1. RoF architecture and spectrally paired down-/uplink.

Concept and Experimental Setup

As a path towards simplification of RRH optics, we adopt a single EML device as an opto-electronic mm-wave transceiver, as discussed in in Fig. 1, together with the corresponding spectral configuration. As demonstrated earlier for the sub-6GHz band [14], coherent homodyne detection of an analogue RoF downlink (DL) signal and transmission of an uplink (UL) RoF signal can be accomplished simultaneously: The optical carrier Λ of the downlink RoF signal is used to injection-lock the distributed feedback (DFB) laser section of the EML. The DFB laser serves as local oscillator $LO_{RRH} \equiv \Lambda$ for coherent homodyne detection of the downlink radio signal. The high-bandwidth (40G rated) electro-absorption modulator (EAM) is not only used as a photodiode but also as the uplink modulator. Crosstalk χ from the orders-of-magnitude stronger uplink signal at the transmit branch of the RRH is mitigated through a paired radio spectrum, which dedicates two different mm-wave carriers to the down-/uplink channels [15], allowing for a directional split implemented by means of frequency division

duplexing (FDD). Additionally, we simplify the analogue RoF reception by means of photonic down-conversion of the uplink mm-wave radio signal to a sub-6GHz carrier frequency at the CO. This is accomplished with a second coherent EML receiver at the head-end, whose LO_{CO} is locked much closer to the uplink OFDM signal through appending a virtual carrier (VC) that is synchronized with the LO_{CO} (rather than the optical uplink carrier Λ). With this, the OFDM signal after photodetection is yielded at a rather low intermediate frequency (IF). This mitigates the need for RF mixers and mm-wave carrier generation. It further renders the double-sideband uplink RoF transmission robust to dispersion-induced penalties because of the filtering of one modulation sideband through the frequency-selective coherent detection.

The experimental setup is shown in Fig. 2a. At the CO, the downlink OFDM signal is up-converted to a mm-wave carrier in the K_a-band and modulated onto an optical carrier at Λ = 1539.2 nm, using a Mach-Zehnder modulator (MZM). A 50/100 GHz interleaver (IL) is inserted to obtain optical single-sideband (SSB) transmission to mitigate dispersion-induced signal fading during downlink photodetection. The signal is then launched through a filterless optical distribution network (ODN) towards the RRH. The ODN is composed by a dual feeder with a length of 14.3 km and a 1-km drop segment, using a circulator as the direction split.

At the RRH, an EML performs the conversion between optical and RF domain through simultaneous coherent downlink detection and uplink transmission, as described earlier. The directional split in the RF domain is performed through a mm-wave diplexer (DPX). At the mobile equipment (ME), the downlink at the higher K_a-band and the uplink in the lower K_a-band are down-/up-converted through RF-based mixers. Wireless transmission between RRH and ME has been omitted to investigate the penalties arising exclusively at the optical layer.

The employed EML is a butterfly-packaged device with a 3dB bandwidth of 33 GHz (Fig. 2a). Its EAM section is biased at -1.2V and the input polarization state of the downlink signal is optimized with a manual polarization controller, though a diversity architecture can be employed to mitigate polarization control [16]. The internal isolator that is co-packaged with the EML prevents efficient downlink detection since it features an isolation of 35.2 dB that we characterized similar as in [17]. For this reason, we have employed an EDFA in the downlink feeder of the ODN to overcome the reverse isolator loss. The received optical power (ROP) is then referred to the optical power level after passing the isolator reversely, at the input of the EAM section (see ROP_{DL} in Fig. 2a). In a practical scenario, where an EML is used without co-packaged isolator, the EDFA could be omitted. Besides, the circulator at the ODN with preceding variable optical attenuator (VOA) would be substituted by a 2×N tree splitter.

At the uplink receiver of the CO, we employ a SOA-preamplified direct-detection PIN receiver with subsequent RF down-converter and an EML-based coherent receiver providing the required means for photonic down-conversion. For the latter, an EDFA is again used to overcome the reverse isolator loss of the employed 10G butterfly EML.

The transmitted mm-wave signal spectra are reported in Fig. 2b for the downlink (δ) at 34.3 GHz and the uplink (υ) at 26.1 GHz. The OFDM signals had 128 sub-carriers over a bandwidth of 500 MHz, which were independently loaded with 16-QAM. Moreover, we append a VC (ς) at 25.8 GHz at a power of +8 dB relative to the OFDM signal, in order to compose a second uplink signal σ at 29.3 GHz for photonic down-conversion to an IF carrier at f_{IF} = 3.5 GHz while ensuring sufficient VC power to lock the EML.

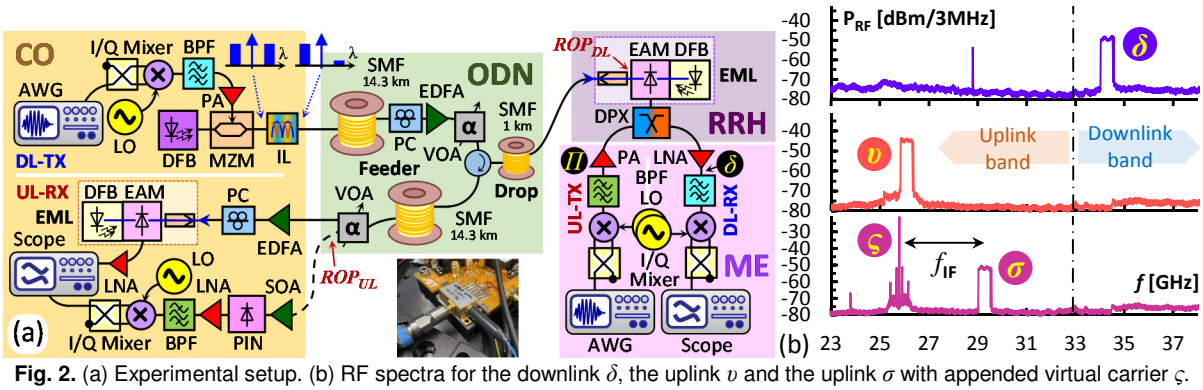

Fig. 2. (a) Experimental setup. (b) RF spectra for the downlink δ, the uplink υ and the uplink σ with appended virtual carrier ς.

Results and Discussion

We have evaluated the down- and uplink performance as a function of the received optical power (ROP) for half- and full-duplex transmission in a back-to-back scenario and with fiber-based ODN. The received RF signal

spectrum in the downlink branch of the RRH (δ in Fig. 2a) is presented in Fig. 3a, together with the two transmission windows T_{DPX} of the mm-wave diplexer used for FDD with a cross-over point at 32.9 GHz. The downlink Δ at 34.3 GHz shows a good SNR after coherent optical signal reception of the analogue RoF signal. When switching on the uplink power amplifier (Π in Fig. 2a) at the diplexer input without applying the uplink OFDM signal, we see the PA background noise π arising at the cross-over point between the up- and downlink bands. Activation of the uplink signal at 26.1 GHz confirms that its crosstalk note χ in the downlink branch of the RRH is well suppressed by the high rejection of >40 dB of the diplexer, resulting in a similar RF power as the downlink. This permits data acquisition without dynamic range limitations.

The downlink EVM is shown in Fig. 3b. We accomplish a low EVM of 4.1% for half-duplex back-to-back (b2b) transmission without uplink (◇). The clean 16-QAM OFDM constellation proves the correct coherent homodyne detection in terms of frequency and phase stability during opto-electronic mm-wave signal conversion at the RRH, which is supported by the low required ROP of -30 dBm to ensure stable locking of the EML for temperature-stabilized DFB emission [12, 17]. The EVM antenna limit at 12.5% is surpassed at -19.8 dBm. In case of full-duplex transmission (△), there is a 0.5% EVM increase at high ROP, while the sensitivity at the EVM limit degrades by 0.4 dB. This confirms the excellent uplink rejection at the directional split of the RRH. With a fiber-populated ODN (◆,▲), we obtain a similar sensitivity as in the back-to-back case. There is no significant dispersion-induced penalty observed due to optical SSB downlink transmission. Even though the EVM at higher ROP levels worsens to 6.1%, the EVM falls still well below the antenna limit.

The uplink EVM is presented in Fig. 3c for direct detection using a SOA+PIN receiver and RF-based down-conversion. We obtain a low EVM of 2.2% for back-to-back transmission for both, half-duplex (□) and full-duplex (○) transmission in presence of a downlink signal. The sensitivity at the EVM antenna limit is -29.7 dBm. However, since no optical SSB filter shall be applied at the RRH transmitter due to complexity considerations, the dispersion-induced fading in the mm-wave band for a fiber-based ODN is significant: It leads to a sensitivity penalty of >6.8 dB at the EVM limit (●,■) and strongly increases the minimum EVM to 8.8%.

We then applied photonic down-conversion at the EML-based coherent homodyne uplink receiver of the CO to select only one of the modulation sidebands of the optical uplink signal while providing frequency translation to an IF in the sub-6GHz range at the same time. Figure 4a presents the spectral configuration for the uplink signal and the LO_{CO} of the EML receiver, which is centered on the lower mm-wave modulation sideband spaced by f_{mm} from the optical carrier Λ. The EML is then optically locked on the VC that has been appended to the uplink OFDM signal (see ς in Fig. 2b), leading to a received OFDM signal that is down-converted to the IF at f_{IF} = 3.5 GHz (see inset in Fig. 4a). The EVM performance is reported in Fig. 4b. Even though the back-to-back reception sensitivity is moderate with -16.2 dBm at the EVM antenna limit (○), which together with the uplink launch of 2.5 dBm from the RRH permits an optical budget of 18.7 dB. Further improvement is expected for chip-based EML samples without isolator. More importantly, we can see that the dispersion-induced penalty has been fully recovered (●). Moreover, the clean 16-QAM OFDM constellations prove the correct optical frequency translation due to joint (*i*) coherent homodyne detection and (*ii*) photonic down-conversion of the mm-wave OFDM signal to an IF of 3.5 GHz without requiring an RF mixer.

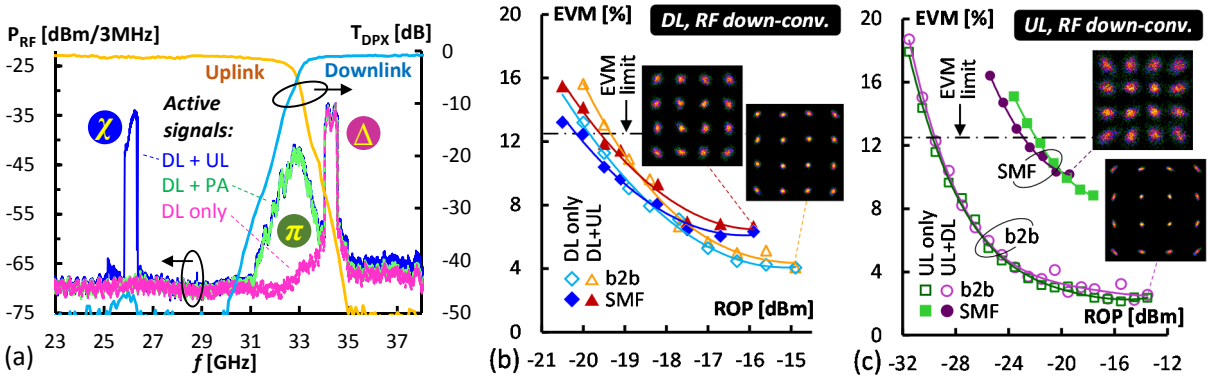

Fig. 3. (a) Received RF spectra at the downlink branch δ of the RRH. (b) Downlink and (c) uplink EVM performance.

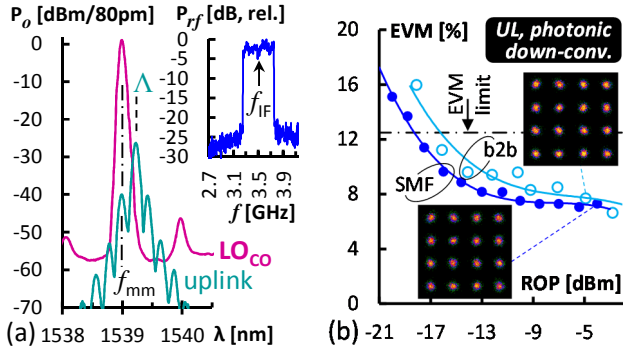

Fig. 4. Photonic f-translation. (a) Uplink spectrum. (b) EVM.

Conclusion

We have demonstrated full-duplex analogue mm-wave radio transmission at 34.3/29.3 GHz over a budget of 18.7 dB and a reach of 15 km, proving good signal integrity and a low EVM in combination with EML transceiver optics and simplified uplink reception involving photonic down-conversion. Scaling up to higher RF bands would require high-bandwidth EAMs, as demonstrated up to 100 GHz. RoF transmission over a filterless ODN permits a smooth wireline-wireless integration in brown-field fiber plants.

Acknowledgements

This work was supported in part by the ERC under the EU Horizon-2020 programme (grant n° 804769) and by the Austrian FFG agency (grant n° 883894).

References

[1] S.A. Busari, K.M.S. Huq, S. Mumtaz, L. Dai, and J. Rodriguez, "Millimeter-Wave Massive MIMO Communication for Future Wireless Systems: A Survey," IEEE Communications Surveys & Tutorials, vol. 20, no. 2, pp. 836-869. 2018. DOI: 10.1109/COMST.2017.2787460

[2] I.A. Alimi, A.L. Teixeira, and P. Monteiro, "Toward an Efficient C-RAN Optical Fronthaul for the Future Networks: A Tutorial on Technologies, Requirements, Challenges, and Solutions," IEEE Communications Surveys & Tutorials, vol. 20, no. 1, pp. 708-769. 2018. DOI: 10.1109/COMST.2017.2773462

[3] K. Zeb, Z. Lu, J. Liu, Y. Mao, G. Liu, P.J. Poole, M. Rahim, G. Pakulski, P. Barrios, M. Vachon, D. Poitras, W. Jiang, J. Weber, X. Zhang, and J. Yao, "Broadband Optical Heterodyne Millimeter-Wave-over-Fiber Wireless Links Based on a Quantum Dash Dual-Wavelength DFB Laser," Journal of Lightwave Technology, vol. 40, no. 12, pp. 3698-3708, 2022. DOI: 10.1109/JLT.2022.3154652

[4] S.R. Moon, M. Sung, J.K. Lee, and S.H. Cho, "Cost-Effective Photonics-Based THz Wireless Transmission Using PAM-N Signals in the 0.3 THz Band," Journal of Lightwave Technology, vol. 39, no. 2, pp. 357-362, 2021. DOI: 10.1109/JLT.2020.3032613

[5] K. Li, and J. Yu, "Photonics-Aided Terahertz-Wave Wireless Communication," Journal of Lightwave Technology, vol. 40, no. 13, pp. 4186-4195, 2022. DOI: 10.1109/JLT.2022.3161878

[6] X. Liu, W. Zhang, J. Yue, D. Lu, F. Yang, and Z. He, "Integrated W-Band Photonic-Wireless Transmitter Enabled by Silicon Microring Modulator and on-Chip Dual-Mode DFB Laser," Proceedings Optical Fiber Communication Conference (OFC), San Diego, United States, Tu3J.6, 2023.

[7] Y. Cai, M. Zhu, J. Zhang, M. Lei, B. Hua, Y. Zou, W. Luo, S. Xiang, L. Tian, J. Ding, L. Ma, Y. Huang, J. Yu, and X. You, "Real-time 100-GbE fiber-wireless seamless integration system using an electromagnetic dual-polarized single-input single-output wireless link at W band," Optics Letters, vol. 48, no. 4, pp. 928-931, 2023. DOI: 10.1364/OL.481386

[8] Y.S. Lin, W.C. Fan, C.J. Lin, C.Y. Li, and H.H. Lu, "Bi-Directional 5G NR Fiber-Wireless Systems With Single-Carrier Optical Modulation and Phase Modulation Scheme," Proceedings Optical Fiber Communication Conference (OFC), San Diego, United States, Tu3J.2, 2023.

[9] W. Li, J. Yu, B. Zhu, J. Zhang, M. Zhu, F. Zhao, T. Xie, K. Wang, Y. Wei, X. Yang, B. Hua, M. Lei, Y. Cai, W. Zhou, and J. Yu, "Photonics-Assisted 320 GHz THz-Band 50 Gbit/s Signal Outdoor Wireless Communication Over 850 Meters," Proceedings Optical Fiber Communication Conference (OFC), San Diego, United States, Th4C.5, 2023.

[10] L. Zhao, K. Wang, and W. Zhou, "Transmission of 4096-QAM OFDM at D-band," Optics Express, vol. 31, no. 2, pp. 2270-2281, 2023. DOI: 10.1364/OE.464283

[11] L. Bogaert, J. Van Kerrebrouck, H. Li, I. Lima de Paula, K. Van Gasse, C.Y. Wu, P. Ossieur, S. Lemey, H. Rogier, P. Demeester, G. Roelkens, J. Bauwelinck, and G. Torfs, "SiPhotonics/GaAs 28-GHz Transceiver With Reflective EAM for Laser-Less mmWave-Over-Fiber," Journal of Lightwave Technology, vol. 39, no. 3, pp. 779-786, 2021. DOI: 10.1109/JLT.2020.3021175

[12] B. Schrenk, and F. Karinou, "World's First TO-can Coherent Transceiver," Proceedings Optical Fiber Communication Conference (OFC), San Diego, United States, Th1A.4, 2018. DOI: 10.1364/OFC.2018.Th1A.4

[13] B. Schrenk, and F. Karinou, "Single-Carrier, Single-λ Full-Duplex Analog Radio Feed over a Single-Port RRH Transceiver," Journal of Lightwave Technology, vol. 41, no. 4, pp. 1114-1121, 2023. DOI: 10.1109/JLT.2022.3230405

[14] B. Schrenk, "The EML as Analogue Radio-over-Fiber Transceiver – a Coherent Homodyne Approach," Journal of Lightwave Technology, vol. 37, no. 12, pp. 2866-2872, 2019. DOI: 10.1109/JLT.2018.2870537

[15] S. Parkvall, E. Dahlman, A. Furuskär, and M. Frenne, "NR: The New 5G Radio Access Technology," IEEE Communications Standards Magazine, vol. 1, no. 4, pp. 24-30, 2017. DOI: 10.1109/MCOMSTD.2017.1700042

[16] B. Schrenk, and F. Karinou, "Simple Laser Transmitter Pair as Polarization-Independent Coherent Homodyne Detector," Optics Express, vol. 27, no. 10, pp. 13942-13950, 2019. DOI: 10.1364/OE.27.013942

[17] B. Schrenk, M. Hofer, and T. Zemen, "Analogue Receiver for Coherent Optical Analogue Radio-over-Fiber Transmission," Optics Letters, vol. 42, no. 16, pp. 3165-3168, 2017. DOI: 10.1364/OL.42.003165